ACS Chemical Neuroscience

Review

pubs.acs.org/chemneuro

Efficiency Gains in Tracer Identification for Nuclear Imaging: Can In Vivo LC-MS/MS Evaluation of Small Molecules Screen for Successful PET Tracers?

Elizabeth M. Joshi,*,† Anne Need, John Schaus, Zhaogen Chen, Dana Benesh, Charles Mitch, Stuart Morton, Thomas J. Raub, Lee Phebus, and Vanessa Barth*

Eli Lilly and Co., Lilly Research Laboratories, Indianapolis, Indiana 46285, United States

ABSTRACT: Positron emission tomography (PET) imaging has become a useful noninvasive technique to explore molecular biology within living systems; however, the utility of this method is limited by the availability of suitable radiotracers to probe specific targets and disease biology. Methods to identify potential areas of improvement in the ability to predict small molecule performance as tracers prior to radiolabeling would speed the discovery of novel tracers. In this retrospective analysis, we characterized the brain penetration or peak SUV (standardized uptake value), binding potential (BP), and brain exposure kinetics across a series of known, nonradiolabeled PET ligands using in vivo LC-MS/MS (liquid chromatography coupled to mass spectrometry) and correlated these parameters with the reported PET ligand performance in nonhuman primates and humans available in the literature. The PET tracers studied included those reported to label G protein-coupled receptors (GPCRs), intracellular enzymes, and transporters. Additionally, data for each tracer was obtained from a mouse brain uptake assay (MBUA), previously published, where blood−brain barrier (BBB) penetration and clearance parameters were assessed and compared against similar data collected on a broad compound set of central nervous system (CNS) therapeutic compounds. The BP and SUV identified via nonradiolabeled LC-MS/MS, while different from the published values observed in the literature PET tracer data, allowed for an identification of initial criteria values we sought to facilitate increased potential for success from our early discovery screening paradigm. Our analysis showed that successful, as well as novel, clinical PET tracers exhibited BP of greater than 1.5 and peak SUVs greater than approximately 150% at 5 min post dose in rodents. The brain kinetics appeared similar between both techniques despite differences in tracer dose, suggesting linearity across these dose ranges. The assessment of tracers in a CNS exposure model, the mouse brain uptake assessment (MBUA), showed that those compound with initial brain-to-plasma ratios >2 and unbound fraction in brain homogenate >0.01 were more likely to be clinically successful PET ligands. Taken together, early incorporation of a LC/MS/MS cold tracer discovery assay and a parallel MBUA can be an useful screening paradigm to prioritize and rank order potential novel PET radioligands during early tracer discovery efforts. Compounds considered for continued in vivo PET assessments can be identified quickly by leveraging in vitro affinity and selectivity measures, coupled with data from a MBUA, primarily the 5 min brain-to-plasma ratio and unbound fraction data. Coupled utilization of these data creates a strategy to efficiently screen for the identification of appropriate chemical space to invest in for radiotracer discovery.

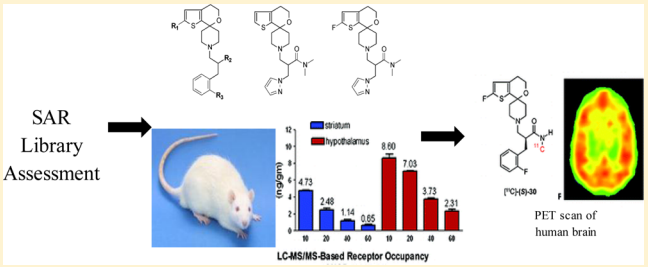

KEYWORDS: *Positron emission tomography (PET), imaging, in vivo, mass spectrometry, rat, biomarker, preclinical translation*

Positron emission tomography (PET) and single-photon emission tomography (SPECT) have been successfully applied to answer a variety of biological questions, including direct measurements of clinical target engagement. In addition to target occupancy measures, radiolabeled imaging tracers have been utilized to measure pharmacodynamic processes, such as cellular metabolism (FDG). Radiotracers have been employed to assess the ability of a compound to occupy the target, to interrogate changes in synaptic tone of endogenous neurotransmitter systems and to investigate changes in receptor number (Bmax) as well as affinity (K_d).[1,2] However, such investigations are limited to the available tools or radiotracers developed for a specific targets or processes. While most of the radiotracer discovery work has focused on the monoaminergic receptors (GPCRs), their synthetic and catabolic enzymes (COMT, MAO), along with their transporter related-mechanisms (SERT, DAT, NET), the identification of novel tracers in other areas such as glutametergic targets, ion channels (beyond the nicotinics), and intracellular enzymes (other than COMT, PDE4) are not as abundant.

Over the past decade there have been significant advances in the mass spectrometry field that have increased the ability of mass spectrometers to detect and quantitate very low levels

Received: April 7, 2014
Revised: September 22, 2014
Published: September 23, 2014

(down to fmol) of analytes across a variety of matrices. As a result of these advances, high performance liquid chromatography coupled to tandem mass spectrometry (LC-MS/MS) has been applied to tracer identification efforts.[3−6] This unique application of technology has been critical in being able to reduce bottlenecks in radiotracer discovery, by enabling the evaluation of nonlabeled small molecules in vivo as potential tracer candidates. By circumventing the need for radiolabeled molecules, this method has directly enabled a decreased turnaround time for in vivo evaluation of a compound's propensity to differential distribute relative to known target biology, assessment of specific and nonspecific binding, brain uptake or SUV, as well as brain and plasma kinetics.[7] As such, this technique enables access to broader chemical space that might not be practicable to evaluate for potential tracers if radiolabeling were required.

One key advantage to the LC-MS/MS approach includes an ability to evaluate numerous compounds quickly in an effort to iterate in vivo tracer data and optimize tracer performance quickly. The early selection of key molecules that possess low nonspecific binding will be more likely to exhibit favorable differential distribution in vivo consistent with the biology, or binding potential. The differential distribution, or binding potential (BP), is directly related to the density of the target (B_{max}) and the affinity of the compound (K_d = dissociation constant) where B_{max}/K_d should be greater than 5.[8] It stands to reason then, that targets with higher expression levels may be easier to tackle versus those with lower expression levels.

Another advantage of the LC-MS/MS technique is the lack of early radioactivity useage. This attribute relieves the environmental and regulatory constraints that are placed on tracer discovery laboratories handling radioactivity. For groups working to identify suitable tracer ligands, an initial investment into a LC-MS/MS system is required; however, this investment is significantly cheaper and less regulated as compared to the investments made for the acquisition and maintenance of, or access to, a cyclotron as well as working with radioactivity for more labor intensive autoradiography and ex vivo binding studies. While the necessity for imaging technology is critical to ultimately evaluating individual tracers, once the most promising candidates have been identified with LC-MS/MS technology, access to these capabilities can be achieved through research collaborations with global partners who have the necessary radiochemistry and imaging expertise. For those institutions already possessing such infrastructure, the application of this technique for radiotracer screening purposes can enable a more efficient use of such radiolabeling and imaging resources.

The use of nonlabeled compounds for tracer screening does have a drawback in that it cannot address the ability to definitively predict radioactive metabolite(s) and their potential ability to confound PET imaging. Radiometabolites, possess two potential fates most efficiently assessed in vivo via PET/SPECT imaging in nonhuman primates or ultimately in man: (1) if the radiometabolites are lipophilic and present in the brain, they can exhibit high nonspecific binding that will decrease the signal-to-noise measurements or (2), if active, may work to compete in binding at the target and will confound measurements because of the inability to discern a signal between parent or metabolite specie. In vitro metabolite profiling of nonradiolabeled ligands can be helpful understanding the potential clearance pathways associated with the molecule and provide context for the imaging data obtained as well as to guide the radiolabeling strategy. In some cases, the measurement of nonlabeled metabolites generated in vivo has been feasible by LC-MS/MS. However, in many circumstances given the low dose of the parent compound, a tracer dose, detection and quantitation has been a challenge. So, while the LC-MS/MS will ultimately increase efficiency in tracer discovery/identification it can by no means replace the need to run in vivo preclinical PET/SPECT imaging studies. This "cold" approach, however, can effectively limit the number of radiolabeled studies needed to ultimately achieve these goals

Central nervous system access, and thus blood brain barrier (BBB) penetration, is needed for radiotracers designed for brain targets. Radiotracers for brain targets require free drug levels to engage the target; however, no set strategy to iterate vast libraries of compounds has been suggested. To this end, we evaluated clinical PET imaging data of a number of known PET ligands (and reverse translated these nonlabeled PET tracers to enable preclinical target engagement assays on the LC-MS/MS platform) in the LC-MS/MS rat tracer assessment. Additionally, we investigated these same PET tracer compounds in an MBUA model to identify a potential strategy to facilitate the discovery of de novo tracers. The LC-MS/MS application coupled with an early in vivo assessment in the MBUA allowed for the prioritization and rank ordering of existing PET ligands with respect to BP and SUV and was able to triage candidate for radiotracer discovery for both nociceptin and kappa opioid receptors.

RESULTS AND DISCUSSION

Early discovery of suitable CNS drug molecules have been achieved primarily through the use of rodent animals models.[9] Given that discovery chemistry teams can design and/or synthesize a diverse set of molecules, being able to effectively prioritizeing compounds for efficacy assessments can be a challenge, especially for analyses within labor intensive animal models. This same conundrum exists in the realm of novel PET tracer discovery given the lengthy time required for radiotracer identification and validation prior to clinical. Efforts to identify a new tracer molecule needs to initiate as early as possible during the drug development process in order to allow sufficient time for thise identification/qualification process. This can be challenging when the characteristics of the therapeutic agent may be sufficiently different from the PET ligand requiring two separate SAR (structure activity relationship) strategies.

To this end, we examined the use of a mouse brain uptake assay (MBUA) to differentiate successful tracer performance as an early screening tool for compounds prior to in vivo preclinical LC-MS/MS evaluations. In that assay suite, in vivo plasma/brain exposure kinetics are examined across 2 defined time points and jointly evaluated with in vitro permeability and unbound fraction measurements in brain homogenates and plasma, as previously published.[10] Table 1 provides a summary of the median results and general physicochemical property comparisons determined across the test of PET tracers and therapeutic compounds for CNS targets. Not surprisingly, the physicochemical properties associated with PET ligands were generally similar to those properties associated with the CNS therapeutic compound space. Consistent with the notion that tracers should have rapid kinetics, all PET ligands evaluated showed a consistently higher loss from both plasma and brain across the 5 and 60 min time interval. Interestingly, the loss from the brain and plasma were noted to be similar suggesting

Table 1. Median Property Analysis of General CNS Therapeutic Compounds versus the Reverse Translated Tracers in the Mouse Brain Evaluation Assay

parameter	PET ligands	CNS data set[b]	comments
no. H-bond donors	1	1	none >2
no. H-bond acceptors	4	5	range: 3−6
polar surface area (Å^2)	51	69	range: 34−70
clogP	3.2	3.2	ChemAxon, Cambridge, MA
clogD pH 7.4	3.0	2.5	ChemAxon, Cambridge, MA
C_{plasma} (nmol/mL)[a], 5 min	1.4	2.8	
C_{brain} (nmol/g)[a], 5 min	3.1	2.6	
C_{plasma} (nmol/mL)[a], 60 min	0.32	0.25	
C_{brain} (nmol/g)[a], 60 min	0.37	0.09	
plasma % loss	94	84	
brain % loss	94	80	
BBB P_{app} (10^{-6} cm/s)	29	8	estimated from 5 min $K_{p,brain}$[10]
$K_{p,brain}$, 5 min	2.1	0.6	
% dose in brain, 5 min	1.6	0.6	Cardiac Output = 1.9%[10]
$C_{brain,u}$ (Nm)	87	37	
$K_{p,uu}$	1.3	3.4	

[a]Mean value. [b]Data set evaluated did not include any compounds considered for cold tracer analysis.

rapid equilibration. Rapid distribution into the CNS was observed among the PET tracers evaluated and data suggested an approximate 3-fold higher apparent blood-brain barrier permeability coefficient or BBB $P_{app.}$ It should be pointed out that while this permeability coefficient appeared to be higher, there exists a wider range of diversity within the CNS compounds evaluated at physiologically relevant dose ranges which is thought to skew the median value, and as such was not utilized as an initial screening parameter for success. There was no attempt in this paper to compare tracers identified with leading CNS candidates across similar targets. After correcting total brain concentrations with the unbound fraction ($f_{u,brain}$) measured using equilibrium dialysis in brain homogenates, the unbound brain concentrations ($C_{brain,u}$) were determined and found to be approximately 2-fold higher (on average) with $f_{u,brain}$ generally being greater than 0.01 for a majority of the tracers. At low tracer doses, maximizing the unbound drug levels for tracer molecules is considered an advantage, especially for targets with low expression levels. Given the inherent variability of protein binding measurements at low f_u regions, it is unknown whether this 2-fold difference is "real" per se, however, a mindset toward ensuring adequate free drug levels in the brain during tracer discovery is viewed by the authors as an advantage and is utilized as an initial screening criteria. The analysis presented herein across the 22 PET tracers, and numerous CNS therapeutic compounds (data not shown), resulted in establishing the following criteria for initial compound selection for in vivo LC-MS/MS tracer assessment

Table 2. Characterization of Established and Novel Tracers Using Nonlabeled Compounds Measured By LC-MS/MS, PET Literature Comparative Analysis and a Preclinical Rodent Brain Exposure Assessment[a]

			preclinical rat uptake		literature PET data			MBUA evaluation			
tracer	target	brain region	LC-MS/MS BP (value, time point)	LC-MS/MS SUV (value, time point)	corresponing BP (value, time point)	corresponding SUV (value, time point)	species PET data obtained	Exp 5 min K_p	Exp $f_{u,brain}$	Exp $f_{u,plasma}$	Exp $K_{p,uu}$
WAY-100635	5-HT1A	hippocampus	20, 40 min	300%, 40 min	6, 40 min	500%, 5 min	human	3.03	0.081	0.161	6.0
MDL-100907	5-HT2A	frontal cortex	2.4 20 min	360%, 5 min	1.5, 40 min	400%, 5 min	human	7.79	0.064	0.389	47.1
R107474	lpha 2A adrenergi	medial septum	2.7, 40 min	300% 20 min	3.2, 30 min	700%, 5 min	rat	3.51	0.026	0.013	1.8
MK9470	CB1	frontal cortex	9.4, 60 min	100%, 60 min	2.3, 60 min	120%, 60 min	human	ND	ND	ND	ND
FMPEP	CB1	frontal cortex	9, 60 min	100%, 15 min	2.6, 30 min	450%, 15 min	human	ND	0.001	0.003	ND
MePPEP	CB1	frontal cortex	6.8, 30 min	130, 15 min	1.3, 60 min	330%, 10 min	human	2.35	0.001	0.002	5.0
Fallypride	D2	striatum	11.5, 40 min	420%, 20 min	11, 40 min	700%, 60 min	human	ND	ND	ND	ND
PHNO	D3/D2	striatum	3.2, 20 min	420%, 20 min	2.5, 60 min	500%, 5 min	human	ND	ND	ND	ND
FECNT	DAT	striaum	6.5, 20 min	597%, 5 min	7.0, 40 min	700%, 5 min		6.18	ND	ND	ND
Flumazenil	GABAA (BZD)	frontal cortex	1.4, 20 min	460%, 5 min	1 0.3, 20 min	500%, 5 min	human	1.54	0.46	0.70	2.4
GSK189254	H3	frontal cortex	2.4, 40 min	86%, 40 min	3.5, 40 min	400%, 5 min	human	1.59	0.35	0.44	2.0
ABP-688	mGluR5	hippocampus	4, 20 min	200%, 20 min	0.9, 20 min	600%, 5 min	human	2.38	0.02	0.02	2.2
SP-203	mGluR5	hippocampus	17, 20 min	220%, 5 min	5.5, 60 min	600%, 5 min	human	14	0.04	0.09	33.8
FITM	mGluR1	cerebellum	2.8, 40 min	600%, 20 min	3, 40 min	500%, 20 min	NHP	ND	ND	ND	ND
NOP 1A	Noc-1	hypothalamus	2.4 40 min	280%, 10 min	1.2, 40 min	600%, 5 min	human	2.81	0.038	0.88	64.2
NOP 2A	Noc-1	hypothalamus	3.8 40 min	450%, 10 min	0.5, 40 min	400%, 5 min	NHP	2.52	0.006	0.005	2.2
NOP 3A	Noc-1	hypothalamus	3.6 40 min	280%, 10 min	1.3, 40 min	500%, 5 min	NHP	3.52	0.155	0.024	0.5
LY2795050	OPRA Kappa	striatum	1.8 40 min	130%, 5 min	1.3, 40 min	250%, 5 min	human	1.2	0.011	0.0052	0.6
GR103545	OPRA Kappa	striatum	1.5, 40 min	130%, 10 min	1.0, 40 min	200%, 30 min	NHP	3.84	0.039	0.314	31.3
N-methyl JDTic	OPRA Kappa	striatum	0.5, 40 min	23%, 20 min	1.4, 30 min	6.40%	rat	0.024	0.020	0.058	0.1
MeNER	NET	thalamus	0.5, 40 min	70%, 20 min	0.4, 40 min	180%, 5 min	NHP	3.9	0.058	0.254	17.2
FDMeNER	NET	thalamus	1.9, 60 min	100%, 20 min	0.5, 40 min	280%, 5 min	NHP	9.27	ND	ND	ND

[a]The preclinical and clinical PET imaging data analysis was based on the available species data obtained. ND = not determined.

dx.doi.org/10.1021/cn500073j | ACS Chem. Neurosci. 2014, 5, 1154−1163

follow-up: 5 min $K_{p,brain}$ > 2 and $f_{u,brain}$ > 0.01. However, during the initial screening iterations, a less stringent 5 min $K_{p,brain}$ is applied with values >0.3. This is consistent with a strategy to first identify the chemical space that yields an in vivo differential distribution, rather than limiting compound evaluation based on potential performance from an SUV perspective.

A selected set of PET tracers commercially available ranging targets such as G protein-coupled receptors (GPCRs), intracellular enzymes, and transporters were carried out using the nonlabeled LC-MS/MS technique and compared to PET imaging evaluations across a wide range or target types of CNS PET ligands. The tracers were selected to represent a variety of target types and illustrate both the ability to reverse translate existing clinical PET tracers and aid in the discovery of de novo tracers for novel targets (Table 2).[11−39] A representative example of the preclinical validation data obtained using our unlabeled LC-MS/MS approach with the dopamine D_2/D_3 tracer FLB-457 is illustrated in Figure 1. In comparison to the

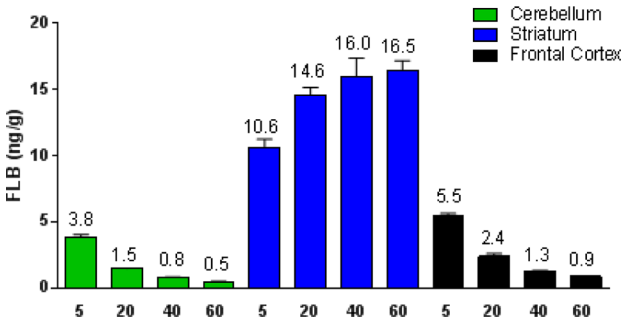

Figure 1. Representative "cold" LC-MS/MS evaluation in rat of the dopamine D2/D3 tracer FLB-457 (n = 4).

published PET data by Farde et al., we observed a similar profile demonstrating slow kinetics, signal-to-noise and uptake for the dopamine D_2/D_3 tracer, FLB-457.[11] In healthy subjects, the striatal uptake of radioactivity was observed to peak around 60 min which is similar to the LC-MS/MS results with nonlableled FLB-457. FLB-457 tracer levels continued to increase, beyond 60 min, but can be seen to flatten out in caudate/putamen or striatum regions. However, in both cortical and cerebellar brain regions FLB-457 uptake is observed to be clearing out 20 min post dose. As such, our tissue time activity/concentration curves for all three brain regions were considered similar across both techniques. This same observation was noted for the binding potentials as well.

Analysis of the data obtained via the "cold" LC-MS/MS method shows that the absolute values for both BP and SUV are different when compared to the published values for the PET tracers; however, when graphed (Figures 2 and 3) a general correlation between nonlabeled and radiolabeled analysis was observed. The statistical analysis of the data demonstrated a moderate positive correlation (Spearman's ρ correlation coefficient of 0.64) suggesting that the LC-MS/MS technique gave a similar rank-order output (p-value of 0.0012). Table 2 provides a summary of LC-MS/MS measured BP and SUV, in addition to the literature comparison. Given that BP and SUV are key in vivo outputs from both the PET imaging and preclinical uptake assessments, via LC-MS/MS, we compared the different detection systems for these values. To compare BP values, the specific time point data, which was matched to the LC-MS/MS data collected, were estimated from the published time-activity curves. The peak SUV values attained within the first hour of the same time-activity curves were compared to the peak SUV values obtained by LC-MS/MS. In our analysis, the "cold" LC-MS/MS data set was able to rank order the PET tracers for both BP and SUV, even though the measurements were made only once per compound (n = 4 animals/expt). It is recognized that a true comparible BP measurement can only be achieved under equilibrium conditions and that our current screening approach may not recapitulate this situation; however, the relationship currently identified across the differing PET ligands evaluated herein suggests an early approach toward rank ordering that improves our ability to identify successful prioritization of novel PET ligands in the clinical, as exemplified with the discovery of the NOP and Kappa tracers by our group.[13,24,40]

By evaluating a variety of clinically validated PET tracers established at multiple imaging centers in this manner, the "cold" LC-MS/MS data collected enabled the identification of minimal perfromace criteria for both BP and SUV for this technique. For instance, the kappa opioid tracers LY2795050 and GR103545 appeared comparable for both BP and SUV as measured by LC-MS/MS. Similar parameters obtained from the literature showed a comparable assessment, as well, despite the acknowledged species differences and differing functional activity (antagonist vs agonist). Interestingly, data from the MBUA assessment showed LY2795050 to have approximately 4-fold higher nonspecific binding as indicated by the low unbound fraction in brain ($f_{u,b} \approx 0.01$) versus GR103545 ($f_{u,b} \approx 0.04$). Measured brain kinetics from the MBUA also indicated an improved CNS partitioning for LY2795050 suggesting improved tracer performance; however, the current techniques employed here to assess nonspecific binding did not take into account the kinetics associated with nonspecific binding. It is suspected that molecules which achieve rapid equilibrium with quick on/off rates may be more able to interact versus those whose equilibrium takes longer to establish, despite a similar measured value. Likewise, the mGluR5 tracers ABP-688 and SP203 demonstrate a larger BP as measured by LC-MS/MS vs corresponding PET measurements where SP203 shows a 4-fold increase in specific binding to mGluR5. This could be a function of measuring the parent tracer only by LC-MS/MS as well as species differences across multiple parameters. A closer evaluation of the raw data demonstrated that SP203 had a larger signal-to-noise than ABP-688 (which also was recapitulated in PET imaging results).[29,34] Both techniques, however, identify low nonspecific specific binding in the null tissue as a factor for the larger binding potential and were able to identify the compounds as potential PET radiotracers. On the other hand, *N*-methyl JD Tic had no specific binding in vivo by LC-MS/MS and exhibited the lowest BP and SUV results measured from the literature. The data analysis in the mouse brain exposure assessment showed that *N*-methyl JD Tic had poor partitioning in the rodent CNS model, along with a high degree of nonspecific binding. These data, coupled with the "cold" LC-MS/MS outcome only are suggestive that this molecule may not perform well as a clinical PET tracer. Preclinical imaging studies in rodents with *N*-methyl JD Tic showed a low degree of uptake into the BBB (consistent with the low partitioning observed in vitro), yet it was sufficient to measure a signal and, as such, the compound was investigated as a potential PET ligand since it was the only antagonist tracer for this target at the time. A priori knowledge of this potential response might have informed investigators of

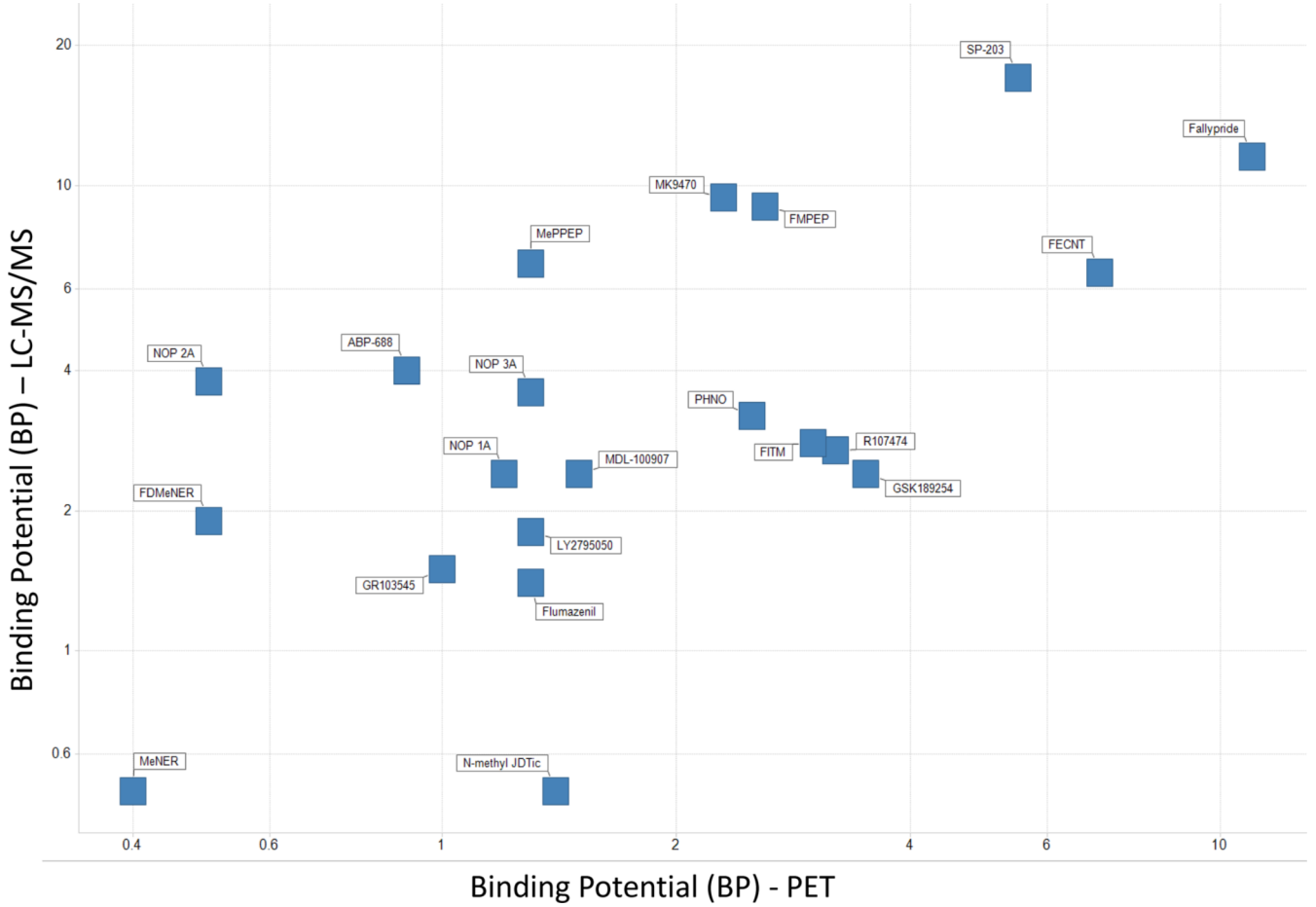

Figure 2. A comparative analysis of the binding potential assessed by LC-MS/MS in vivo evaluation of nonlabeled tracers (*y*-axis) versus binding potential values found in the literature (*x*-axis) from various clinical PET tracer experiments. Compounds are labeled by Tracer name as outlined in Table 2. Statistics characterizing the relationship were evaluated and are as follows: p value = 0.0012, Spearman ρ = 0.645, pairwise correlation = 0.78, R^2 = 0.6.

this outcome and reserved the imaging resources undertaken and spent additional time to identify additional promising molecules or projects.

As previously mentioned, identifying molecules with high unbound brain concentrations can be important when looking for potential PET tracers. At low tracer doses, achieving an adequate degree of unbound drug to label available targets, coupled with appropriate kinetics (washout from brain by 60–90 min) would be beneficial toward identifing a tracer molecule able to differentially distribute. An application of the free-drug hypothesis and success in the PET tracer field can be best as exemplified by evaluating the Kappa opioid antagonist ligands LY2795050, LY2459989, and *N*-methyl JDTic.[25,27,38,40] Specifically, $K_{p,uu}$, a measure for the extent of free distribution in the CNS, was estimated to be approximately 0.6, 1.2 versus 0.1, respectively, for each ligand. This measurable difference is thought to be one potential reason for the improved performance of the LY2459989 relative to LY2795050, as well as for both LY tracers in comparison to *N*-methyl JDTic. While the initial screening criteria is articulated for a total partitioning coefficient, K_p, an assessment of the unbound partitioning is also a closely monitored parameter during our selection process.

A thorough review of the data collected across the 22 PET tracers (Table 2) surveyed has suggested the following guidelines currently utilized as a screening paradigm for novel tracer discovery: MBUA 5 min $K_{p,brain} > 2$ and $f_{u,brain} > 0.01$, BP values greater than 1.5 and peak SUV values of greater than approximately 150% post-tracer dose in rodent LC-MS/MS studies enabled a positively predicted PET tracer response in higher order species. This strategy, at a minimum, can be utilized to select a very narrow chemical space, or identify the most promising 2–3 molecules, to focus on translating into nonhuman primate imaging studies thereby reducing the compounds requiring radiochemical syntheses, obviating the rodent PET, and reducing the resourcing of higher-order species PET imaging. As exemplified with the kappa antagonist tracer example described above, the joint analysis of data across a variety of early discovery assays demonstrates a potential strategy to screen for PET radiotracers.

While the LC-MS/MS technique appears to help identify or screen potential PET tracers, there are still a number of caveats to consider. For instance, in the case of species differences in target affinity, the LC-MS/MS technique and rodent PET studies can be irrelevant and may require moving directly to a higher order species as early as possible. Another consideration arises related to the species-specific metabolism that must be acknowledged since this LC-MS/MS application may not predict radiometabolite liability in subsequent PET analyses. For example, in the case of tracer discovery efforts for the NOP receptor, *N*-demethylation was observed as a primary route of clearance for the leading preclinical tracer molecule.[13] To

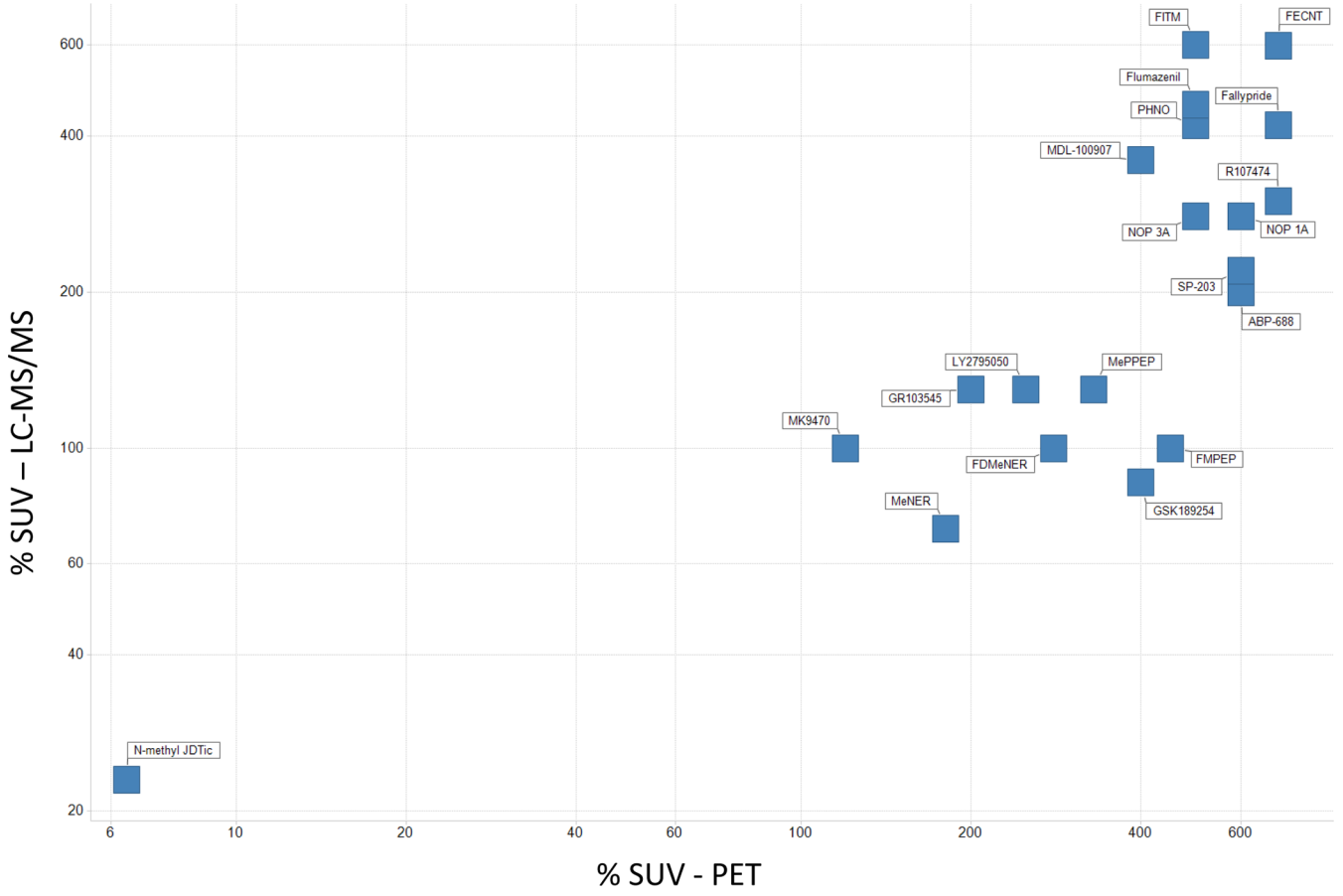

Figure 3. A comparative analysis of the % SUV assessed by LC-MS/MS in vivo evaluation of nonlabeled tracers (y-axis) versus % SUV values found in the literature (x-axis) at comparable time points from various clinical PET tracer experiments. Compounds are labeled by tracer name as outlined in Table 2. Statistics characterizing the relationship were evaluated and are as follows: p value = 0.0099, Spearman ρ = 0.538, pairwise correlation 0.62, R^2 = 0.4.

reduce the potential for radiometabolite formation, additional demethylated analogs were evaluated in primate PET studies. The ultimate PET tracer, NOP1A, selected for clinical use was a monodesmethyl analog with good brain penetration, favorable kinetics, and high receptor-specific signaling.

Admittedly, this analysis is focused on a small data set since only radiotracers that were clinically established were used for reverse translation purposes. This was done with a focus toward the creation of an "ideal" radiotracer composite profile. Potential molecules being evaluated as tracers that do not perform well regardless of technique employed do not move forward for PET imaging, and are lacking as suitable negative controls. This lack of negative control compounds to compare against is especially problematic for understanding issues associated with poor SUV, especially where compounds with ABC transporter or poor liphophilicity may not be fully examined by PET imaging. A retrospective review of the performance of *N*-methyl JD Tic as a tracer is a classic example where limited chemical space was available (at the time) for the development of a kappa antagonist PET tracer, yet now that improved chemical space has been identified two enhanced PET ligands have now been published (e.g.,·LY2459989 and LY2795050).[24,38,40] Looking from a forward translational perspective, only a small number of successful compounds that were evaluated in PET imaging were included in this review. One of the advantages of the "cold" LC-MS/MS technique is the ability to identify compounds that differentially distribute in tissue matching target expression as a primary output very early in the discovery process. This ability to differentially distribute in such a microdosing paradigm is the most important factor and is what makes a tracer unique versus the identification of the therapeutic compound for development. The ability to preselect compounds with a higher likelihood of performing in such a manner, and then the ability to rapidly test this in vivo enables the discovery of novel tracers and most importantly identifies the best chemical space for subsequent design and optimization to take place.

Zhang et al. recently published on an approach using a CNS multiparameter optimization (CNS MPO) design tool to enrich the design and selection of successful novel PET ligands which is primarily focused on the design of successful compounds using calculated physiochemical properties.[43] Internally, we have extended the same methodology to our internal data set of tracers and see an approximate 50% success rate. Taking a specific look at the 22 tracers outlined in Table 3, the identification of successful ligands is slightly increased (~60%) but this single criteria alone would limit the potential development of current clinically successful tracers like the NOP-1 and κ-opioid receptor ligands.[13,40] Careful attention to the relationship of in silico modeled parameters, such as logP and logD, to measured results within SAR space is deemed useful for success in the design phase, but is not considered robust enough to select the most promising of in vivo candidates.

dx.doi.org/10.1021/cn500073j | *ACS Chem. Neurosci.* 2014, 5, 1154−1163

Table 3. Predicted Properties and CNS PET MPO for 22 Reviewed PET Ligands

tracer	target	clogP (Chemaxon)	clogD (Chemaxon, pH7.4)	MW	TPSA (Novartis)	HBD	pK_a, most basic (Chemaxon)	CNS MPO score[a]
N-methyl JDTic	OPRA Kappa	4	2.74	479.66	76	3	9.55	0.75
NOP 2A	Noc-1	4.45	3.03	462.6	32.8	0	8.82	1.71
FMPEP	CB1	5.51	4.46	472.48	41.6	1	8.41	2.04
MePPEP	CB1	5.33	4.28	454.49	41.6	1	8.41	2.04
MK9470	CB1	5.87	5.87	489.59	84.2	1	3.18	2.35
LY2795050	OPRA Kappa	3.84	2.85	407.9	68.5	1	8.35	2.53
GR103545	OPRA Kappa	2.64	1.57	414.33	53.1	0	8.44	2.62
WAY-100635	5-HT1A	4.17	4.08	531.95	48.9	0	6.74	2.95
NOP 3A	Noc-1	3.92	2.71	436.98	41.6	1	8.59	3.09
FECNT	DAT	3.32	3.19	325.81	29.5	0	6.92	3.21
MDL-100907	5-HT2A	3.59	2.23	373.47	41.9	1	8.75	3.27
NOP 1A	Noc-1	3.46	2.13	420.52	41.6	1	8.72	3.70
R107474	alpha 2A adrenergic	2.47	0.978	359.43	50.8	0	8.88	3.76
GSK189254	H3	3.11	1.11	351.45	54.5	1	9.4	3.89
FITM	mGluR1	3.75	3.75	371.44	71	1	2.38	4.26
Fallypride	D2	2.81	2.17	514.54	50.8	1	7.93	4.35
SP-203	mGluR5	3.34	3.34	260.27	36.7	0	−0.288	4.45
FDMeNER	NET	3.1	2.47	433.39	39.7	1	7.91	4.87
ABP-688	mGluR5	3.02	3.02	240.3	34.5	0	4.21	4.90
PHNO	D3/D2	2.88	2.46	283.8	32.7	1	7.6	5.04
MeNER	NET	2.92	2.29	335.82	39.7	1	7.91	5.06
Flumazenil	GABAA (BZD)	0.128	0.128	303.29	64.4	0	3.27	5.90

[a]See ref 43 for calculation of CNS MPO using predicted properties.

The strategy suggested herein leverages the MBUA along with appropriate in silico tools (as internally developed) to identify suitable chemical space for de novo tracer evaluation, which can be screened by "cold" LC-MS/MS for further prioritization toward PET ligand discovery.[7,41,42] This aproach extends the field's current practice of relying soly on both calculated and measured cLogP data to assess lipophilicy as a primary driver for selecting compounds that would be expected to differentially distribute in vivo.[43] Continued advancement in this field is necessary and will no doubt expand our selection of suitable biomarkers to evaluate target engagement and disease biology in areas not yet adequately characterized. Beyond the approaches discussed, other methods believed to enhance discovery efforts in this area include the potential for cassette dosing during the tracer screening process and the extension of biomathematical modeling approaches to understand key interactions in key organs of interest (namely CNS for neuroscience).[44,45]

In summary, the combination of these techniques and preclinical in vivo models permit a rapid, cost-effective mechanism for de novo tracer discovery. Utilizing a nonlabeled LC-MS/MS-based approach reduces the need for preclinical PET imaging studies, while allowing for increased exploration of the chemical space from which to identify new tracers and permits the entry of other participants in the search for new radiotracers. The application of HPLC-MS/MS, coupled with MBUA, in radiotracer discovery can lead to expedited and, ultimately, more available PET ligands for clinical research.

METHODS

Test Compounds. The following compounds were purchased from ABX Advanced Biochemical Compounds (ABX GmbH, Germany): altanserin (LSN 3056580), setoperone (LSN 2358766), beta-CIT (LSN 3043689), FLB 457 (LSN 2358756), and FECNT (LSN 3043755). WAY 100635, flumazenil, and DASB were purchased from Sigma-Aldrich (St. Louis, MO, USA). MK 9470, MICA, MDL 100907, FMPEP, MePEPP, SP203, FPEB, ABP, MeNER, FDMeNER, GR103545, LY2456302, *N*-methyl JDTic, LSN2459989, LSN2839434, LSN2839546, LSN2874428, LY2428703, LY2459989, and LY2795050 were synthesized at Eli Lilly and Company. All compounds were formulated as a 1 mg/mL solution and diluted with various vehicles compatible for intravenous dosing prior to dosing low enough to be (1) considered a tracer dose (<10 μg/kg) and (2) reliably quantified by LC-MS/MS.

Animals. Adult male Sprague−Dawley rats (Harlan Laboratories, Indianapolis, IN, USA) weighing approximately 220−300 g were housed six to a cage in a room using a 12-h on/off lighting schedule (lights on at 6AM). Room temperature was maintained at 21 ± 3 °C. Animals had ad libitum access to food and water and were permitted to adapt to housing conditions at least 2 days after arrival at our site before testing. Tracer compounds were examined in groups of 4 rats that were briefly restrained and injected with nonlabeled tracer in the lateral tail vein. Animals were sacrificed by cervical dislocation. After sacrifice, brain regions appropriate for the target biology were dissected and weighed. These regions included a high target expressing region as well as a low/no expressing brain region.

Analysis of Unlabeled Tracer Levels. Previously weighed brain tissue samples were placed in conical 1.5 mL polypropylene centrifuge tubes and 4 volumes (w/v) of acetonitrile containing 0.1% formic acid were added. Samples were then homogenized using an ultrasonic dismembrator probe (Fisher Scientific model 100, Pittsburgh, PA, USA), vortexed and centrifuged for 16 min at 16 000 × *g* (Eppendorf model 5417R, Westbury, NY, USA). Supernatant samples were

diluted with sterile water to generate samples with less acetonitrile than contained in the LC mobile phase and vortexed.

Tracer concentration were measured using a liquid chromatography system (HPLC, Agilent Technologies model 1100, Wilmington, DE, USA) coupled with triple quadrapole mass spectral detection. The HPLC system employed a C18 column (2.1 mm × 50 mm; Agilent; part no. 971700-907) with an aqueous mobile phase consisting of acetonitrile with 0.1% formic acid and a flow rate of 0.4 mL/min. Tracers were quantified after elution from the HPLC column using an API 4000 triple-quad mass spectrometer (Applied Biosystems, Foster City, CA, USA) in positive electrospray mode using multiple reaction monitoring (MRM) methods to monitor the transition from parent to daughter ions. Chromatographic assays were calibrated using a standard curve generated by extracting a series of brain tissue samples from nontreated animals to which known quantities of analyte had been added. Binding potentials were calculated as the ratio of (total binding (ng/g)/nonspecific binding (ng/g)) − 1 based on the well-established ratio method.[8]

Statistical Analyses. Prism (GraphPad Software Inc., version 4.0, San Diego, CA) software was employed for calculations, curve fitting and graphics. JMP (SAS Institute Inc., version 8.0, Cary, NC) was used for all statistical calculations comparing the PET and LC-MS/MS readouts (Figures 1 and 2).

Plasma and whole brain homogenate protein binding in mouse. The extent of protein binding was determined in vitro by equilibrium dialysis using a HTDialysis 96-well, 150-μL half-cell capacity, Teflon equilibrium dialysis plate and cellulose membranes (12−14 kDa molecular weight cutoff) (HTDialysis LLC; Gales Ferry, CT) as described elsewhere.[43] Either plasma with K2EDTA as the anticoagulant (Lampire Biological laboratories, Pipersville, PA), adjusted to pH 7.4 with phosphoric acid immediately prior to use, or mouse or rat brain homogenate was used. Brain homogenate was prepared in 100 mM phosphate buffer (1:3, w/v; pH 7.4) by probe sonication. Matrices were spiked with DMSO stock solutions of test compounds to give final concentrations of 0.1% DMSO and 1 μM compound. Initial plasma and brain homogenate concentrations were determined by LC−MS/MS as described below. Compound-spiked brain homogenate or plasma were placed into the donor chambers of the dialysis plate (100 μL per half-well), and an equal volume of phosphate buffer (100 mM, pH 7.4) was placed in each corresponding receiver well (n = 3/compound/matrix). The dialysis plate was sealed with the kit adhesive and dialysis was conducted on an orbital shaker (175 rpm) at 37 °C for 4.5 h. Following incubation, donor and receiver chamber compound concentrations were determined by LC-MS/MS. Brain homogenate, plasma, and dialysate samples were prepared for bioanalysis by methanol protein precipitation. Fraction unbound (f_u) values were calculated as the ratio of the receiver chamber (buffer) concentration and the donor chamber concentration. Fraction unbound brain was determined by correcting the values in brain homogenate for the 3-fold dilution of brain tissue with phosphate buffer.[44] Fraction unbound data were acceptable when compound recovery was 100 ± 30%.

Mouse Brain Uptake Assessment (MBUA). A simplified, calibrated mouse brain uptake assay (MBUA) has been described in detail elsewhere.[10] Mice were acclimated for 1 week prior to use at 23 ± 1 g bodyweight. Nonfasted mice were dosed intravenously by tail vein injection with 50-μL containing 55 nmole (2.2 μmol/kg) test compound in 8:2 (w/w) 1,2-propanediol:DMSO. At 5 and 60 min postinjection, plasma samples, from blood collected in tubes containing K2EDTA as the anticoagulant, and brain cerebral hemispheres were immediately frozen and stored at −80 °C until bioanalysis. Samples were thawed with 2:1 (v/v for plasma or v/wt for brain) addition of 1:9 (v/v) tetrahydrofuran:acetonitrile and brain samples were homogenized using a Model 100 Sonic Dismembrator (Fisher Scientific, Pittsburqh, PA) prior to removal of precipitated proteins by centrifugation and injection of 1 μL of the supernatant onto the column. Brain concentrations were corrected for an average measured plasma volume of 16 μL/g brain tissue.[10] The unbound brain partition coefficient ($K_{p,uu}$) was approximated by correcting the 5 min measured $K_{p,brain}$ ($C_{brain,total}/C_{plasma,total}$ or 5 min brain-to-plasma ratio) with the experimentally determined unbound fractions as follows:

$$K_{p,uu} \approx (\text{5-min } K_{p,brain})(f_{u,p}/f_{u,b})$$

AUTHOR INFORMATION

Corresponding Authors

*E-mail: elizabeth.joshi@merck.com (E.M.J.).

*E-mail: barth_vanessa_nicole@lilly.com (V.B.).

Present Address

†E.M.J.: Merck and Company, Merck Research Laboratories, 2000 Galloping Hill Road, K15F-2107, Kenilworth, NJ 07033, USA..

Notes

The authors declare no competing financial interest.

ABBREVIATIONS

PET, positron emission tomography; LC-MS/MS, liquid chromatography coupled to tandem mass spectrometry; SUV, standardized uptake value (typically expressed as a percentage); BP, binding potential; B_{max}, maximal binding capacity; K_d, steady state dissociation constant; GPCR, G-protein coupled receptor; FDG, fluoro deoxyglucose; BBB, blood−brain barrier; CNS, central nervous system; MBUA, mouse brain uptake assessment;

REFERENCES

(1) Dewey, S. L., Smith, G. S., Logan, J., Brodie, J. D., Simkowitz, P., MacGregor, R. R., Fowler, J. S., Volkow, N. D., and Wolf, A. P. (1993) Effects of central cholinergic blockade on striatal dopamine release measured with positron emission tomography in normal human subjects. *Proc. Natl. Acad. Sci. U. S. A. 90*, 11816−20.

(2) Gallezot, J. D., Kloczynski, T., Weinzimmer, D., Labaree, D., Zheng, M. Q., Lim, K., Rabiner, E. A., Ridler, K., Pittman, B., Huang, Y., Carson, R. E., Morris, E. D., and Cosgrove, K. P. (2014) Imaging nicotine- and amphetamine-induced dopamine release in rhesus monkeys with [(11)C]PHNO vs [(11)C]raclopride PET. *Neuropsychopharmacology 39*, 866−74.

(3) Barth, V. N., Chernet, E., Martin, L. J., Need, A. B., Rash, K. S., Morin, M., and Phebus, L. A. (2006) Comparison of rat dopamine D2 receptor occupancy for a series of antipsychotic drugs measured using radiolabeled or nonlabeled raclopride tracer. *Life Sci. 78*, 3007−3012.

(4) Chernet, E., Martin, L. J., Li, D., Need, A. B., Barth, V. N., Rash, K. S., and Phebus, L.A. (2005) Use of LC/MS to assess brain tracer distribution in preclinical, in vivo receptor occupancy studies: Dopamine D2, serotonin 2A and NK-1 receptors as examples. *Life Sci. 78*, 340−346.

(5) Pike, V. W., Rash, K. S., Chen, Z., Pedregal, C., Statnick, M. A., Kimura, Y., Hong, J., Zoghbi, S. S., Fujita, M., Toledo, M. A., Diaz, N., Gackenheimer, S. L., Tauscher, J. T., Barth, V. N., and Innis, R. B. (2011) Synthesis and evaluation of radioligands for imaging brain nociceptin/orphanin FQ peptide (NOP) receptors with positron emission tomography. *J. Med. Chem. 54*, 2687−700.
(6) Donohue, S. R., Krushinski, J. H., Pike, V. W., Chernet, E., Phebus, L., Chesterfield, A. K., Felder, C. C., Halldin, C., and Schaus, J. M. (2008) Synthesis, ex vivo evaluation, and radiolabeling of potent 1,5-diphenylpyrrolidin-2-one cannabinoid subtype-1 receptor ligands as candidates for in vivo imaging. *J. Med. Chem. 51*, 5833−42.
(7) Barth, V., and Need, A. (2014) Identifying novel radiotracers for PET imaging of the brain: Application of LC-MS/MS to tracer identification. *ACS Chem. Neurosci.*, DOI: 10.1021/cn500072r.
(8) Meunier, J. C., M?llereau, C., Toll, L., Suaudeau, C., Moisand, C., Alvinerie, P., Butour, J. L., Guillemot, J. C., Ferrara, P., Monsarrat, B., Mazarguil, H., Vassart, G., Parmentier, M., and Costentin, J. (1995) Isolation and structure of the endogenous agonist of opioid-like ORL 1 receptor. *Nature 377*, 532−535.
(9) Desai, P. V., Sawada, G. A., Watson, I. A., and Raub, T. J. (2013) Integration of in silico and in vitro tools for scaffold optimization during drug discovery: predicting P-glycoprotein efflux. *Mol. Pharmaceutics 10*, 1249−61.
(10) Raub, T. J., Lutzke, B. S., Andrus, P. K., Sawada, G. A., and Staton, B. A. (2006) Early preclinical evaluation of brain exposure in support of hit identification and lead optimization, in *Optimizing the "Drug-Like" Properties of Leads in Drug Discovery, Biotechnology: Pharmaceutical Aspects Series* (Borchardt, R. T., and Middaugh, C. R., Eds,), pp 355−410, Springer, New York.
(11) Farde, L., Suhara, T., Nyberg, S., Karlsson, P., Nakashima, Y., Hietala, J., and Halldin, C. (1997) A PET-study of [11C]FLB 457 binding to extrastriatal D2-dopamine receptors in healthy subjects and antipsychotic drug-treated patients. *Psychopharmacology (Berlin, Ger.) 133*, 396−404.
(12) Siméon, F. G., Liow, J. S., Zhang, Y., Hong, J., Gladding, R. L., Zoghbi, S. S., Innis, R. B., and Pike, V. W. (2012) Synthesis and characterization in monkey of [11C]SP203 as a radioligand for imaging brain metabotropic glutamate 5 receptors. *Eur. J. Nucl. Med. Mol. Imaging 39*, 1949−58.
(13) Pedregal, C., Joshi, E. M., Toledo, M. A., Lafuente, C., Diaz, N., Martinez-Grau, M. A., Jiménez, A., Benito, A., Navarro, A., Chen, Z., Mudra, D. R., Kahl, S. D., Rash, K. S., Statnick, M. A., and Barth, V. N. (2012) Development of LC-MS/MS-based receptor occupancy tracers and positron emission tomography radioligands for the nociceptin/orphanin FQ (NOP) receptor. *J. Med. Chem. 55*, 4955−4967.
(14) Atack, J. R., Scott-Stevens, P., Beech, J. S., Fryer, T. D., Hughes, J. L., Cleij, M. C., Baron, J. C., Clark, J. C., Hargreaves, R. J., and Aigbirhio, F. I. (2007) Comparison of lorazepam [7-chloro-5-(2-chlorophenyl)-1,3-dihydro-3-hydroxy-2*H*-1,4-benzodiazepin-2-one] occupancy of rat brain gamma-aminobutyric acid(A) receptors measured using in vivo [3*H*]flumazenil (8-fluoro 5,6-dihydro-5-methyl-6-oxo-4*H*-imidazo[1,5-*a*][1,4]benzodiazepine-3-carboxylic acid ethyl ester) binding and [11C]flumazenil micro-positron emission tomography. *J. Pharmacol. Exp. Ther. 320*, 1030−7.
(15) Burns, H. D., Van Laere, K., Sanabria-Bohórquez, S., Hamill, T. G., Bormans, G., Eng, W. S., Gibson, R., Ryan, C., Connolly, B., Patel, S., Krause, S., Vanko, A., Van Hecken, A., Dupont, P., De Lepeleire, I., Rothenberg, P., Stoch, S. A., Cote, J., Hagmann, W. K., Jewell, J. P., Lin, L. S., Liu, P., Goulet, M. T., Gottesdiener, K., Wagner, J. A., de Hoon, J., Mortelmans, L., Fong, T. M., and Hargreaves, R. J. (2007) [18F]MK-9470, a positron emission tomography (PET) tracer for in vivo human PET brain imaging of the cannabinoid-1 receptor. *Proc. Natl. Acad. Sci. U. S. A. 104*, 9800−5.
(16) Chang, Y. S., Jeong, J. M., Yoon, Y. H., Kang, W. J., Lee, S. J., Lee, D. S., Chung, J. K., and Lee, M. C. (2005) Biological properties of 2′-[18F]fluoroflumazenil for central benzodiazepine receptor imaging. *Nucl. Med. Biol. 32*, 263−8.
(17) Cropley, V. L., Innis, R. B., Nathan, P. J., Brown, A. K., Sangare, J. L., Lerner, A., Ryu, Y. H., Sprague, K. E., Pike, V. W., and Fujita, M. (2008) Small effect of dopamine release and no effect of dopamine depletion on [18F]fallypride binding in healthy humans. *Synapse 62*, 399−408.
(18) Davis, M. R., Votaw, J. R., Bremner, J. D., Byas-Smith, M. G., Faber, T. L., Voll, R. J., Hoffman, J. M., Grafton, S. T., Kilts, C. D., and Goodman, M. M. (2003) Initial human PET imaging studies with the dopamine transporter ligand 18F-FECNT. *J. Nucl. Med. 44*, 855−61.
(19) Elmenhorst, D., Minuzzi, L., Aliaga, A., Rowley, J., Massarweh, G., Diksic, M., Bauer, A., and Rosa-Neto, P. (2010) In vivo and in vitro validation of reference tissue models for the mGluR(5) ligand [(11)C]ABP688. *J. Cereb. Blood Flow Metab. 30*, 1538−49.
(20) Farde, L., Ito, H., Swahn, C. G., Pike, V. W., and Halldin, C. (1998) Quantitative analyses of carbonyl-carbon-11-WAY-100635 binding to central 5-Hydroxytryptamine-1A receptorsin man. *J. Nucl. Med. 39*, 1965−1971.
(21) Graff-Guerrero, A., Mizrahi, R., Agid, O., Marcon, H., Barsoum, P., Rusjan, P., Wilson, A. A., Zipursky, R., and Kapur, S. (2009) The dopamine D2 receptors in high-affinity state and D3 receptors in schizophrenia: A clinical [11C]-(+)-PHNO PET study. *Neuropsychopharmacology 34*, 1078−86.
(22) Logan, J., Carruthers, N. I., Letavic, M. A., Sands, S., Jiang, X., Shea, C., Muench, L., Xu, Y., Carter, P., King, P., and Fowler, J. S. (2012) Blockade of the brain histamine H3 receptor by JNJ-39220675: Preclinical PET studies with [(11)C]GSK189254 in anesthetized baboon. *Psychopharmacology (Berlin, Ger.) 223*, 447−55.
(23) (a) Lohith, T. G., Zoghbi, S. S., Morse, C. L., Araneta, M. F., Barth, V. N., Goebl, N. A., Tauscher, J. T., Pike, V. W., Innis, R. B., and Fujita, M. (2012) Brain and whole-body imaging of nociceptin/orphanin FQ peptide receptor in humans using the PET ligand 11C-NOP-1A. *J. Nucl. Med. 53*, 385−92. (b) Masilamoni, G., Votaw, J., Howell, L., Villalba, R. M., Goodman, M., Voll, R. J., Stehouwer, J., Wichmann, T., and Smith, Y. (2012) (18)F-FECNT: Validation as PET dopamine transporter ligand in parkinsonism. *Exp. Neurol. 226*, 265−73.
(24) Mitch, C. H., Quimby, S. J., Diaz, N., Pedregal, C., de la Torre, M. G., Jimenez, A., Shi, Q., Canada, E. J., Kahl, S. D., Statnick, M. A., McKinzie, D. L., Benesh, D. R., Rash, K. S., and Barth, V. N. (2011) Discovery of aminobenzyloxyarylamides as κ opioid receptor selective antagonists: application to preclinical development of a κ opioid receptor antagonist receptor occupancy tracer. *J. Med. Chem. 54*, 8000−8012.
(25) Poisnel, G., Oueslati, F., Dhilly, M., Delamare, J., Perrio, C., Debruyne, D., and Barré, L. (2008) [11C]-MeJDTic: A novel radioligand for kappa-opioid receptor positron emission tomography imaging. *Nucl. Med. Biol. 35*, 561−9.
(26) Ryzhikov, N. N., Seneca, N., Krasikova, R. N., Gomzina, N. A., Shchukin, E., Fedorova, O. S., Vassiliev, D. A., Gulyás, B., Hall, H., Savic, I., and Halldin, C. (2005) Preparation of highly specific radioactivity [18F]flumazenil and its evaluation in cynomolgus monkey by positron emission tomography. *Nucl. Med. Biol. 32*, 109−16.
(27) Schoultz, B. W., Hjornevik, T., Willoch, F., Marton, J., Noda, A., Murakami, Y., Miyoshi, S., Nishimura, S., Arstad, E., Drzezga, A., Matsunari, I., and Henriksen, G. (2010) Evaluation of the kappa-opioid receptor-selective tracer [(11)C]GR103545 in awake rhesus macaques. *Eur. J. Nucl. Med. Mol. Imaging 37*, 1174−80.
(28) Schou, M., Zoghbi, S. S., Shetty, H. U., Shchukin, E., Liow, J. S., Hong, J., Andrée, B. A., Gulyás, B., Farde, L., Innis, R. B., Pike, V. W., and Halldin, C. (2009) Investigation of the metabolites of (S,S)-[(11)C]MeNER in humans, monkeys and rats. *Mol. Imaging Biol. 11*, 23−30.
(29) Shetty, H. U., Zoghbi, S. S., Siméon, F. G., Liow, J. S., Brown, A. K., Kannan, P., Innis, R. B., and Pike, V. W. (2008) Radiodefluorination of 3-fluoro-5-(2-(2-[18F](fluoromethyl)-thiazol-4-yl)-ethynyl)benzonitrile ([18F]SP203), A radioligand for imaging brain metabotropic glutamate subtype-5 receptors with positron emission tomography, occurs by glutathionylation in rat brain. *J. Pharmacol. Exp. Ther. 327*, 727−35.

(30) Takano, A., Gul yás, B., Varrone, A., and Halldin, C. (2000) Comparative evaluations of norepinephrine transporter radioligands with reference tissue models in rhesus monkeys: (*S*,*S*)-[18F]-FMeNER-D2 and (*S*,*S*)-[11C]MeNER. *Eur. J. Nucl. Med. Mol. Imaging 36* (11), 1885−91.
(31) Talvik-Lotfi M., Nyberg S., Nordström A. L., Ito H., Halldin C., Brunner F., Farde L. High 5HT2A receptor occupancy in M100907-treated schizophrenic patients. *Psychopharmacology (Berlin, Ger.) 148*, 400−3.
(32) Terry, G. E., Liow, J. S., Zoghbi, S. S., Hirvonen, J., Farris, A. G., Lerner, A., Tauscher, J. T., Schaus, J. M., Phebus, L., Felder, C. C., Morse, C. L., Hong, J. S., Pike, V. W., Halldin, C., and Innis, R. B. (2009) Quantitation of cannabinoid CB1 receptors in healthy human brain using positron emission tomography and an inverse agonist radioligand. *Neuroimage 48*, 362−70.
(33) Terry, G. E., Hirvonen, J., Liow, J. S., Zoghbi, S. S., Gladding, R., Tauscher, J. T., Schaus, J. M., Phebus, L., Felder, C. C., Morse, C. L., Donohue, S. R., Pike, V. W., Halldin, C., and Innis, R. B. (2010) Imaging and quantitation of cannabinoid CB1 receptors in human and monkey brains using (18)F-labeled inverse agonist radioligands. *J. Nucl. Med. 5*, 112−20.
(34) Treyer, V., Streffer, J., Ametamey, S. M., Bettio, A., Bläuenstein, P., Schmidt, M., Gasparini, F., Fischer, U., Hock, C., and Buck, A. (2008) Radiation dosimetry and biodistribution of 11C-ABP688 measured in healthy volunteers. *Eur. J. Nucl. Med. Mol. Imaging 35*, 766−70.
(35) Van der Mey, M., Windhorst, A. D., Klok, R. P., Herscheid, J. D., Kennis, L. E., Bischoff, F., Bakker, M., Langlois, X., Heylen, L., Jurzak, M., and Leysen, J. E. (2006) Synthesis and biodistribution of [11C]R107474, A new radiolabeled alpha2-adrenoceptor antagonist. *Bioorg. Med. Chem. 14*, 4526−34.
(36) Yamasaki, T., Fujinaga, M., Maeda, J., Kawamura, K., Yui, J., Hatori, A., Yoshida, Y., Nagai, Y., Tokunaga, M., Higuchi, M., Suhara, T., Fukumura, T., and Zhang, M. R. (2012) Imaging for metabotropic glutamate receptor subtype 1 in rat and monkey brains using PET with [18F]FITM. *Eur. J. Nucl. Med. Mol. Imaging 39*, 632−41.
(37) Zanotti-Fregonara, P., Barth, V. N., Liow, J. S., Zoghbi, S. S., Clark, D. T., Rhoads, E., Siuda, E., Heinz, B. A., Nisenbaum, E., Dressman, B., Joshi, E., Luffer-Atlas, D., Fisher, M. J., Masters, J. J., Goebl, N., Kuklish, S. L., Morse, C., Tauscher, J., Pike, V. W., and Innis, R. B. (2013) Evaluation in vitro and in animals of a new 11C-labeled PET radioligand for metabotropic glutamate receptors 1 in brain. *Eur. J. Nucl. Med. Mol. Imaging 40*, 245−253.
(38) Zheng, M. Q., Nabulsi, N., Kim, S. J., Tomasi, G., Lin, S. F., Mitch, C., Quimby, S., Barth, V., Rash, K., Masters, J., Navarro, A., Seest, E., Morris, E. D., Carson, R. E., and Huang, Y. (2013) Synthesis and evaluation of 11C-LY2795050 as a κ-opioid receptor antagonist radiotracer for PET imaging. *J. Nucl. Med. 54*, 455−466.
(39) Zoghbi, S. S., Shetty, H. U., Ichise, M., Fujita, M., Imaizumi, M., Liow, J. S., Shah, J., Musachio, J. L., Pike, V. W., and Innis, R. B. (2006) PET imaging of the dopamine transporter with 18F-FECNT: A polar radiometabolite confounds brain radioligand measurements. *J. Nucl. Med. 47*, 520−7.
(40) Zheng, M. Q., Kim, S. J., Holden, D., Lin, S. F., Need, A., Rash, K., Barth, V., Mitch, C., Navarro, A., Kapinos, M., Maloney, K., Ropchan, J., Carson, R. E., and Huang, Y. (2014) An improved antagonist radiotracer for the κ-opioid receptor: Synthesis and characterization of 11C-LY2459989. *J. Nucl. Med.*, No. 24854795.
(41) Spreafico, M., and Jacobson, M. (2013) In silico prediction of brain exposure: drug free fraction, unbound brain to plasma concentration ratio and equilibrium half-life. *Curr. Top Med. Chem. 13* (7), 813−820.
(42) Waterhouse, R. N. (2003) Determination of lipophilicity and its use as a predictor of blood−brain barrier penetration of molecular imaging agents. *Mol. Imaging Biol. 5*, 376−89.
(43) Zhang, L., Villalobos, A., Beck, E., Bocan, T., Chappie, T., Chen, L., Grimwood, S., Heck, S., Helal, C., Hou, X., Humphrey, J., Hu, J., Skaddan, M., McCarthy, T., Verhoest, P., Wager, T., and Zasadny, K. (2013) Design and selection parameters to accelerate the discovery of novel central nervous system positron emission tomography (PET) ligands and their application in the development of a novel phosphodiesterase 2A PET ligand. *J. Med. Chem. 56*, 4568−79.
(44) Need, A., McKinzie, J., Mitch, C., Statnick, M., and Phebus, L. (2007) In vivo rat brain opioid receptor binding of LY255582 assessed with a novel method using LC/MS/MS and the administration of three tracers simultaneously. *Life Sci. 81*, 1389−1396.
(45) Guo, Q., Brady, M., and Gunn, R. (2009) A biomathmatical modeling approach to central nervous system radioligand discovery and development. *J. Nucl. Med. 50* (10), 1715−1723.